Scattering theory of topological phase transitions

Fulga, I.C.

Chapter 1

Introduction

1.1 Preface

In 1958 Anderson showed that a quantum particle may be localized by disorder, due to the presence of impurities for instance, even if classically localization does not occur [1]. At fixed disorder strength and energy, all quantum states are either localized or delocalized. This insight provides one of the fundamental ingredients for understanding metals and insulators, as well as the transitions that can take place between these states of matter, now known as Anderson transitions [2].

In the decades that followed, metal-insulator transitions were associated with second-order phase transitions by the advent of field-theoretical descriptions of localization [3, 4], as well as the development of one-parameter scaling theory [5]. The latter assumed the existence of a single variable which would describe both the metallic and the insulating properties of a system close to the phase transition. These properties were expected to fall within certain universality classes, in which the behavior of the conductivity and localization length at the critical point would only depend on the dimensionality and symmetries of the system, irrespective of microscopic details.

Besides providing a means of describing the way in which metals turn insulating or vice versa, the scaling theory of localization was also applied to the quantum Hall effect [6]. Systems showing this effect are not metals, but they are not insulating either, exhibiting localized bulk states and extended edge states at the same time. It was nevertheless understood that the transition between different Hall plateaus was a

localization-delocalization transition, which made scaling theory a useful tool in its description. This was unexpected at the time, since the theory in its original form predicted the absence of extended states in two-dimensional systems [5].

In recent years it was realized that the quantum Hall effect is not the only example of a system with an insulating bulk and a conducting edge [7]. In 2005, Kane and Mele showed that graphene in the presence of spin-orbit interaction has robust, extended edge states, protected by time-reversal symmetry [8]. Many proposals followed, making use of spin-orbit interaction, superconductivity, magnetism, and combinations thereof, leading to the rapid development of what is now known as the field of topological insulators and superconductors [9, 10].

Such systems have been predicted to exist in any spatial dimension and are protected by a variety of symmetries, ranging from the originally proposed one, time-reversal, to crystallographic symmetries of the underlying lattice [11], and even symmetries which are not exact, but only present on average (Chapter 7 of this thesis). Several examples have been experimentally observed [12, 13], and the search for potential applications is one of the most active areas of condensed matter research today. Perhaps the most tantalizing is the possibility of using Majorana fermions, edge states which appear in one-dimensional topological superconductors, as the building blocks for decoherence-free quantum computers [14–16].

The discovery of such a wide range of novel phases of matter calls for the characterization of their physical properties, and of the conditions under which they can appear. Transport signatures are experimentally accessible observables, intensely investigated in the search for Majorana fermions [17–19]. Given this connection, it is natural to make use yet again of the scaling theory of localization to describe the nature and universality classes associated with transitions to and between topological phases of matter.

On a more general level, the correspondence between the presence of a bulk insulating gap and conducting boundary states in topological insulators was initially understood in terms of topological band theory [8, 20], which is based on translational symmetry. More often than not however, this symmetry is broken by the presence of impurities, resulting in a disordered system. It is therefore meaningful to seek alternative descriptions, one of which, scattering theory, is the main focus of this

thesis.

In the following, we will provide a brief description of the main tools used throughout this work, such as the scattering matrix, the topological invariant and the scaling theory of localization. While not aiming to be self-contained, it will provide the basic concepts, as well as relevant references.

1.2 The scattering matrix

The scattering matrix is one of the central objects of study in this thesis. It can be used to describe many transport features at low temperatures, voltages, and frequencies, whenever interactions between particles are either absent, or treated at the mean-field level [21, 22]. Electronic conduction through a mesoscopic sample can be understood in terms of the transmission probabilities of electrons through a that sample, probabilities which can be determined from the scattering matrix [23–27].

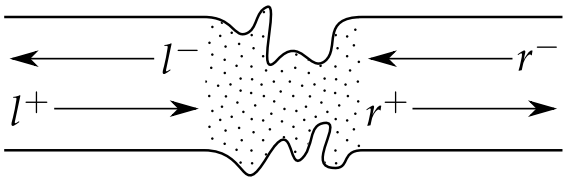

Figure 1.1. Central disordered region connected by means of ideal leads to electron reservoirs (not shown). The modes in the left and right leads are labeled with coefficients $l^{\pm}$ and $r^{\pm}$, depending on their propagation direction.

To introduce it we will closely follow Ref. [22]. Consider a disordered, phase coherent region connected to two electron reservoirs by means of ideal leads, as shown in Fig. 1.1. Far away from the disordered region, in the translationally invariant ideal leads, the wave function of a particle at the Fermi energy E_F can be written in terms of the basis states

$$\psi_n^{\pm} = \phi_n \exp(ik_n x),$$

where ϕ_n is the transversal component, k is the momentum along the translationally invariant direction of the lead, and $n = 1, \ldots, N$ indexes the states, also known as propagating modes, or scattering channels. Particles incident on the disordered region both from the left and right

leads of Fig. 1.1, can be expressed in this basis in terms of coefficients, which we group in the vector

$$\psi_{\text{in}} = (l_1^+, \ldots, l_N^+, r_1^-, \ldots, r_N^-)^T.$$

Here, $\pm$ denotes the sign of the state's velocity, and T stands for transposition. In an analogous fashion, particles leaving the disordered region can also be characterized by a vector of coefficients:

$$\psi_{\text{out}} = (l_1^-, \ldots, l_N^-, r_1^+, \ldots, r_N^+)^T.$$

The scattering matrix relates the vectors ψ_{in} and ψ_{out}:

$$\psi_{\text{out}} = S\psi_{\text{in}}.$$

It is common to express it in terms of its block structure,

$$S = \begin{pmatrix} r & t \\ t' & r' \end{pmatrix}, \tag{1.1}$$

where r (r') contain the probability amplitudes for a particle to be reflected back into the left (right) lead, and t', t are composed of probability amplitudes for transmission from left to right and vice versa. The matrix S is unitary, meaning that its adjoint is equal to its inverse, $S^\dagger = S^{-1}$, owing to current conservation. It is also subjected to other constraints depending on the symmetries of the scattering region, many of which are highlighted in Chapters 2 and 3.

Conductance at zero temperature can be written in terms of the transmission probability of electrons through a sample

$$G = G_0 \text{tr}\, tt^\dagger = G_0 \text{tr}\, t't'^\dagger, \tag{1.2}$$

where the second equality sign is a consequence of the unitarity of S, and G_0 is the conductance quantum, which in the case of electrical transport is e^2/h.

Expressions like Eq. (1.2) carry over also to the case of superconductors, where charge is not a good quantum number, and G then refers to heat conductance through the sample. Finally, the block structure of S can be further exploited to analyze specific scattering processes.

An example used in this thesis is Andreev conductance [28], the charge transfer process by which a current in the metallic lead is converted to a supercurrent in the superconducting region. To express it

in terms of the scattering matrix, it is convenient to introduce an additional grading and consider scattering processes of electrons and holes separately. Each of the reflection blocks in Eq. (1.1) then reads

$$r = \begin{pmatrix} r_{ee} & r_{eh} \\ r_{he} & r_{hh} \end{pmatrix}, \tag{1.3}$$

where $r_{ee(hh)}$ represent the usual electron (hole) reflection. The off-diagonal blocks $r_{eh(he)}$ describe the process of Andreev reflection, by which an incoming electron is converted into a Cooper pair inside the superconductor, and a hole is reflected back out. Given this grading, the Andreev conductance is written as [29, 30]

$$G/G_0 = N - \operatorname{tr} r_{ee} r_{ee}^\dagger + \operatorname{tr} r_{eh} r_{eh}^\dagger, \tag{1.4}$$

with N the number of propagating modes in the metallic lead.

In Chapter 6, Andreev conductance is used to adaptively tune a system to a spot in parameter space where the topologically non-trivial phase is most robust.

1.3 Topological invariants

A system is called a topologically non-trivial insulator (or superconductor) whenever it is insulating in the bulk, but has a fixed number of gapless states at its surface. These conducting boundary states are *topologically protected*, which means that deformations of the system or its parameters will not remove any of them as long as the bulk stays insulating, and as long as certain symmetries are preserved.

The first known example of such a system is the integer quantum Hall effect [31]. When a two-dimensional electron gas is subjected to a strong magnetic field, the quantized electron cyclotron orbits lead to the formation of highly degenerate energy levels, called Landau levels. Whenever the Fermi energy lies between two levels, the bulk of the system is insulating. However, the edges are not. one way to visualize this behavior is to imagine classical trajectories of electrons close to the boundary, called *skipping orbits* (see Fig. 1.2).

A remarkable feature of these systems is that the existence and robustness of the conducting edge states is actually a property of the insulating bulk. This bulk-boundary correspondence ensures that even

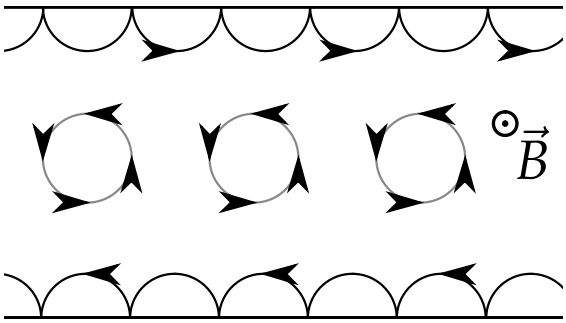

Figure 1.2. Two-dimensional electron gas placed in a strong magnetic field $\vec{B}$. The electrons in the center of the sample have localized, classical cyclotron orbits, whereas those close to the boundary reflect off of it, forming so called skipping orbits which contribute to transport.

if the system is cut into multiple pieces, as long as the bulk gap is not closed, then each individual piece will behave just like the whole, having conducting states along its surface.

It is natural to ask whether one can write down an expression which counts the number of edge states starting only from the bulk. In 1982, Thouless, Kohmoto, Nightingale, and den Nijs did just that [32], deriving a quantity now known as the TKNN invariant. Given a translationally invariant two-dimensional bulk characterized by Bloch wave functions $|u_\alpha(\mathbf{k})\rangle$, this integer, also known as the Chern number, reads

$$n_\alpha = \frac{1}{2\pi} \int d^2\mathbf{k}\ \nabla \times i\langle u_\alpha(\mathbf{k})|\nabla_\mathbf{k}|u_\alpha(\mathbf{k})\rangle. \tag{1.5}$$

Physically, the above quantity may be understood in terms of the Berry phase [33] of the wave functions $|u_\alpha(\mathbf{k})\rangle$. When adiabatically evolved over a closed loop in momentum space, they acquire a geometric phase given by

$$\gamma_\alpha = \oint_\mathcal{C} d\mathbf{k} \cdot i\langle u_\alpha(\mathbf{k})|\nabla_\mathbf{k}|u_\alpha(\mathbf{k})\rangle.$$

When the contour of integration $\mathcal{C}$ extends over the entire Brillouin zone, one can use Stokes' theorem to express it as a surface integral over the Brillouin zone, which leads to the expression (1.5).

It is now known that the quantum Hall effect is but one of multiple possible topological insulators. This has triggered an active interest

in finding new expressions for topological invariants which would apply to these new systems, in finding more efficient expressions, or even approximations. The main focus of Chapters 2 and 3 is to write down expressions for topological invariants which can be efficiently evaluated, and which do not require translational invariance.

1.4 Finite size scaling

According to the single parameter scaling hypothesis [5], the conductance of a system having a linear size L depends on all microscopic details through a single quantity, ξ. This parameter is called correlation length, or localization length, depending on whether one describes a metal or an insulator. The dimensionless conductance is a function of the ratio between these lengths, $g(L/\xi)$, given a dimensionality and a set of symmetries obeyed by the system. With varying system size, the flow of the dimensionless conductance can be described within the scaling theory of localization by the equation

$$\frac{d\ln g}{d\ln L} = \beta(g). \tag{1.6}$$

In other words, the logarithmic derivative of the conductance depends on the conductance itself, and the functional form of this dependence is given by the *beta function*, $\beta(g)$.

In metals, larger samples will exhibit more conductance, meaning $\beta > 0$, while in insulators $g \sim \exp(-L/\xi)$ (and therefore $\beta < 0$), since all wave functions are localized as

$$|\psi(\mathbf{r})|^2 \sim \exp(-|\mathbf{r} - \mathbf{r_0}|/\xi). \tag{1.7}$$

This implies that exactly at the transition between an insulating and a metallic phase, $\beta = 0$ and the conductance of the system, called *critical conductance*, is scale invariant. Additionally, the localization length ξ of Eq. (1.7) must diverge at the transition point, its behavior being parametrized by a *critical exponent*, ν. For a system parameter α (strength of disorder, chemical potential, etc.) that tunes between a metallic and an insulating phase, with a transition at the critical point α_c, the localization length diverges as one approaches the transition as

$$\xi \sim |\alpha - \alpha_c|^{-\nu}. \tag{1.8}$$

One expects the critical exponent ν to be universal, meaning that for a given dimensionality and set of system symmetries, it should not depend on microscopic details.

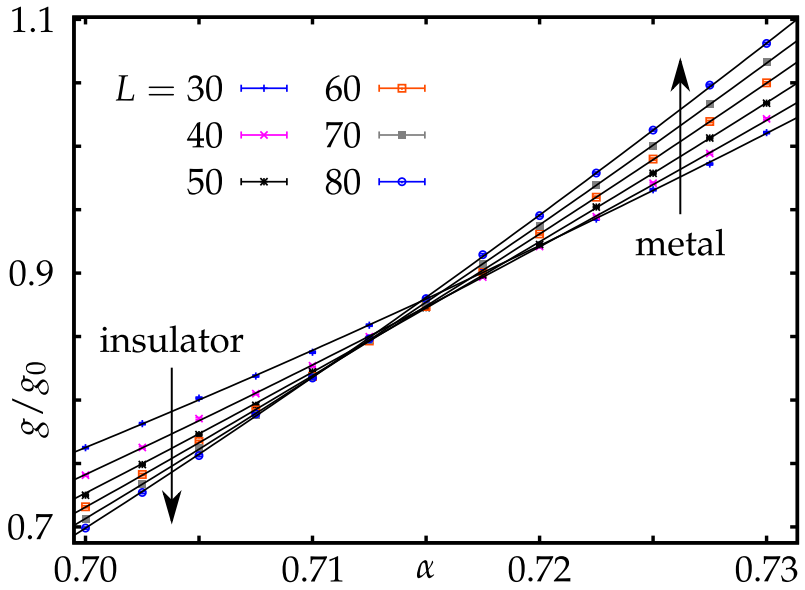

Figure 1.3. Conductance of the model studied in Chapter 5 as a function of a parameter tuning through a metal to insulator phase transition, α. On the left side of the plot, the conductance decreases with system size, $\beta < 0$, so the system is in an insulating phase, whereas on the right side it shows the opposite behavior, $\beta > 0$, indicating a metallic phase. The curves do not intersect at the same point on the plot due to finite size corrections. This apparent shift in the value of the transition point needs to be taken into account when fitting the data (black lines).

The single parameter scaling hypothesis however is only valid in the limit of large system sizes, and in practice finite size corrections can occur [34]. They may manifest themselves as apparent shifts in the values of the critical point α_c and of the critical conductance as a function of L (see Fig. 1.3). Whenever they appear, an accurate determination of the universal properties of a phase transition requires systematically taking these corrections into account. This should be done by considering both the effect of non-linearities on the relevant scaling variable, and the presence of irrelevant scaling variables, which vanish in the large L limit.

In Chapters 4 and 5, two transitions are considered, and the critical

exponent is computed for each one.

1.5 This thesis

In the following, we will give a brief summary of the contents of each thesis chapter.

1.5.1 Chapter 2

The topological quantum number $\mathcal{Q}$ of a superconducting or chiral insulating wire counts the number of protected bound states at the end points. We determine $\mathcal{Q}$ from the matrix r of reflection amplitudes from one of the ends, generalizing the known result in the absence of time-reversal and chiral symmetry to all five topologically non-trivial symmetry classes.

The formula takes the form of the determinant, Pfaffian, or matrix signature of r, depending on whether r is a real matrix, a real antisymmetric matrix, or a Hermitian matrix. We apply this formula to calculate the topological quantum number of N coupled dimerized polymer chains, including the effects of disorder in the hopping constants.

The scattering theory relates a topological phase transition to a conductance peak of quantized height and with a universal (symmetry class independent) line shape. Two peaks which merge are annihilated in the superconducting symmetry classes, while they reinforce each other in the chiral symmetry classes.

1.5.2 Chapter 3

The topological invariant of a topological insulator (or superconductor) is given by the number of symmetry-protected edge states present at the Fermi level. Despite this fact, established expressions for the topological invariant require knowledge of all states below the Fermi energy.

Here we propose a way to calculate the topological invariant employing solely its scattering matrix at the Fermi level, without knowledge of the full spectrum. Generalizing the work done in Chapter 2 for quantum wires, we provide a dimensional reduction recipe which allows to compute topological invariants in higher dimensions.

The approach based on scattering matrices requires much less information than Hamiltonian-based approaches (surface versus bulk), so it is numerically more efficient. Since our formulation is not based on translational symmetry, as is the case when using topological band theory, it is also more naturally suited to the study of disordered systems. Additionally, it provides a direct connection between the topological invariant of a system and its transport properties, leading to novel signatures of topological phase transitions, as will be discussed in the next chapter.

Finally, this method provides us with a new way of visualizing topological phase transitions. In many cases, the invariant can be determined by examining the zeros and poles of the reflection matrix determinant, $\det r$, when applying twisted boundary conditions to the system. Across the phase transition, capturing the evolution of the zeros and poles, in movie format for instance [35], allows to determine "by eye" the symmetries of the system, the point at which the invariant changes, as well as possible re-entrant behavior.

1.5.3 Chapter 4

The conductance of a two-dimensional electron gas at the transition from one quantum Hall plateau to the next has sample-specific fluctuations as a function of magnetic field and Fermi energy. Here we identify a universal feature of these mesoscopic fluctuations in a Corbino geometry: The amplitude of the magnetoconductance oscillations has an e^2/h resonance in the transition region, signaling a change in the topological quantum number of the insulating bulk.

One way of understanding how this occurs relates back to the previous chapter. The change of invariant across the plateau transition can be visualized in terms of the evolution of the zeros and poles of $\det r$ under twisted boundary conditions. A zero implies the existence of a fully transmitted bulk mode, which passes through the system exactly at the phase transition point, for the right twist angle.

In a Corbino geometry, varying the magnetic field and Fermi energy, besides tuning through plateau transitions, also has the effect of winding the twist angle. Therefore, along each line separating different quantum Hall phases there is a quasi-periodic conductance resonance, corresponding to the fully transmitted bulk mode.

This resonance also provides a scaling variable for the critical exponent of the phase transition. By looking at $\det r$ and its zeros, one can determine when the phase transition happens and on which side of the transition the system is. Using this information, we construct a scaling variable which is signed, in contrast to the positive-definite ones usually studied in the context of the quantum Hall effect (the conductance or Lyapunov exponents). Remarkably, the scaling variable yields a value for the critical exponent consistent with previous work, but without the need to correct for finite size effects in the form of irrelevant exponents.

1.5.4 Chapter 5

Two-dimensional superconductors with time-reversal symmetry have a $\mathbb{Z}_2$ topological invariant, that distinguishes phases with and without helical Majorana edge states.

In this chapter we perform conductance scaling with varying system size using a model belonging to symmetry class DIII, in order to map its phase diagram. The latter consists of insulating regions, where the thermal conductance decreases with increasing system size, separated by metallic ones, in which larger samples have more conductance.

Using single parameter scaling theory, we determine the universal features across the metal-insulator transitions, finding a critical exponent $\nu \approx 2.0$, about twice the known value in a chiral superconductor. In order to give an accurate estimate, we take into account finite size effects both in the form of non-linearities of the relevant scaling variable, as well as in irrelevant scaling exponents.

Transport properties determine both the phase diagram, as well as the universal features of the model. Additionally, given the results of Chapter 3, they also allow us to compute the topological invariant. Therefore, the system we study is introduced directly in terms of its scattering matrix, as opposed to a tight-binding model: it is a *network model*.

1.5.5 Chapter 6

As mentioned previously, one of the most sought after applications of topological superconductors is the use of Majorana fermions, particles which are their own anti-particles, as building blocks for quantum

computers. Majoranas were predicted to occur as end states of one-dimensional topological superconductors, and could be identified by their transport signature: a conductance peak at zero bias voltage. There are many theoretical proposals to realize them, and recent experimental works have observed a zero bias peak in superconducting quantum wires (see Fig.1.4).

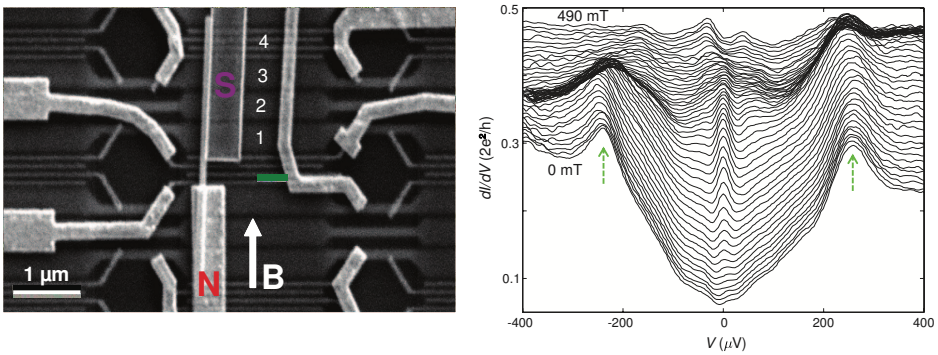

Figure 1.4. Left panel: experimental setup, showing a nanowire coupled to a superconductor (S) and subjected to an external magnetic field (B). A normal metal lead (N) is attached, so that conductance measurements can be performed. Right panel: conductance of the system as a function of bias voltage, for different magnetic field strengths. For a range of magnetic fields, the curves show a zero bias peak, an indicator for Majorana fermions. Taken from Ref. [17], and reproduced with permission from AAAS.

However, given the complex, hard to tune, disordered nature of the considered systems, it is hard to identify this peak exclusively with Majorana physics. Several proposals exist which reproduce similar transport signatures in the absence of topologically protected end states.

We propose a way of overcoming these obstacles by constructing a one-dimensional topological superconductor in a bottom-up fashion, as a linear array of quantum dots. In this way, we gain the ability to separately tune each dot, as well the coupling between them. With a high degree of control over system sub-components, one can unambiguously tune the system to a point deep in the non-trivial phase, with well-localized Majorana fermions at its ends.

In our setup, conductance measurements serve not only to indicate the presence of Majoranas, but are a vital part of the tuning process. Andreev conductance spectroscopy tells us how each sub-component

behaves, and which parameters to address at every step of the adaptive tuning procedure.

1.5.6 Chapter 7

The quantum Hall effect studied in Chapter 4 has topologically protected edge states, in the sense that a perturbation cannot remove these states as long as the bulk gap is maintained. Such a definition carries over to other topological insulators, but additionally requires that system symmetries be preserved. For example, the model studied in Chapter 5 is protected by both particle-hole and time-reversal symmetry. If any of the two is broken, then it becomes possible to smoothly deform the system and remove the edge states.

In this chapter, we study the robustness of edge states when the symmetries protecting them are broken. The question is of particular significance in the case of topological insulators protected by symmetries of the lattice: translations, mirror, or rotations for instance. In any realistic experimental setup, impurities will lead to a breaking of lattice symmetries, and therefore also of edge state protection.

Remarkably, we find that the edge states survive as long as the symmetry is preserved on average. This allows us to define a class of insulators with gapless surface states protected from localization due to the statistical properties of a disordered ensemble, rather than the exact symmetries of each individual sample.

We show that these insulators are topological, being characterized by a $\mathbb{Z}_2$ invariant, and provide a general recipe for their construction using an average mirror symmetry. This significantly extends the list of possible non-trivial phases, as every topological insulator gives rise to an infinite number of classes of "statistical topological insulators" in higher dimensions.

Bibliography

[1] P. W. Anderson, Phys. Rev. **109**, 1492 (1958).

[2] F. Evers and A. D. Mirlin, Rev. Mod. Phys **80**, 1355 (2008).

[3] P. A. Lee and T. V. Ramakrishnan, Rev. Mod. Phys. **57**, 287 (1985).

[4] B. Kramer and A. MacKinnon, Rep. Prog. Phys. **56**, 1469 (1993).

[5] E. Abrahams, P. W. Anderson, D. C. Licciardello, and T. V. Ramakrishnan, Phys. Rev. Lett. **42**, 673 (1979).

[6] B. Huckestein, Rev. Mod. Phys. **67**, 357 (1995).

[7] S. Ryu, A. Schnyder, A. Furusaki, and A. Ludwig, New J. Phys. **12**, 065010 (2010).

[8] C.L. Kane and E.J. Mele, Phys. Rev. Lett. **95**, 226801 (2005).

[9] M. Z. Hasan and C. L. Kane, Rev. Mod. Phys. **82**, 3045 (2010).

[10] X.-L. Qi and S.-C. Zhang, Rev. Mod. Phys. **83**, 1057 (2011).

[11] L. Fu, Phys. Rev. Lett. **106**, 106802 (2011).

[12] M. König, S. Wiedmann, Christoph Brüne, A. Roth, H. Buhmann, L. W. Molenkamp, X.-L. Qi, and S.-C. Zhang, Science **318**, 766 (2007).

[13] D. Hsieh, D. Qian, L. Wray, Y. Xia, Y. S. Hor, R. J. Cava, and M. Z. Hasan, Nature **452**, 970 (2008).

[14] C. Nayak, S. H. Simon, A. Stern, M. Freedman, S. Das Sarma, Rev. Mod. Phys. **80**, 1083 (2008) .

[15] J. Alicea, Rep. Prog. Phys. **75**, 076501 (2012).

[16] C. W. J. Beenakker, Annu. Rev. Con. Mat. Phys. **4**, 113 (2013).

[17] V. Mourik, K. Zuo, S. M. Frolov, S. R. Plissard, E. P. A. M. Bakkers, and L. P. Kouwenhoven, Science **336**, 1003 (2012).

[18] M. T. Deng, C. L. Yu, G. Y. Huang, M. Larsson, P. Caroff, and H. Q. Xu, Nano Lett. **12**, 6414 (2012).

[19] A. Das, Y. Ronen, Y. Most, Y. Oreg, M. Heiblum, and H. Shtrikman, Nat. Phys. **8**, 887 (2012).

[20] B. A. Bernevig, T. L. Hughes, and S. C. Zhang, Science **314** (2006).

[21] C.W.J. Beenakker and H. van Houten, Solid State Physics **44**, 1 (1991).

[22] C. W. J. Beenakker, Rev. Mod. Phys. **69**, 731 (1997).

[23] R. Landauer, IBM J. Res. Dev. **1**, 223 (1957).

[24] R. Landauer, Z. Phys. B **68**, 217 (1987).

[25] Y. Imry, *Directions in Condensed Matter Physics*, World Scientific, Singapore (1986).

[26] M. Büttiker, Phys. Rev. Lett. **57**, 1761 (1986).

[27] M. Büttiker, IBM J. Res. Dev. **32**, 317 (1988).

[28] A. F. Andreev, Sov. Phys. JETP **19**, 1228 (1964).

[29] A. L. Shelankov, JETP Lett. **32**, 122 (1980).

[30] G. E. Blonder, M. Tinkham, and T. M. Klapwijk, Phys. Rev. B **25**, 4515 (1982).

[31] K. von Klitzing, G. Dorda, and M. Pepper, Phys. Rev. Lett. **45**, 494 (1980).

[32] D. J. Thouless, M. Kohmoto, M. P. Nightingale, and M. den Nijs, Phys. Rev. Lett. **49**, 405 (1982).

[33] M. V. Berry, Proc. R. Soc. Lond. A **392**, 45 (1984).

[34] K. Slevin and T. Ohtsuki, Phys. Rev. Lett. **82**, 382 (1999) .

[35] Movies of the zeros and poles of the reflection matrix determinant in three different symmetry classes, across their respective phase transitions, can be found at http://arxiv.org/src/1106.6351v4/anc. A detailed explanation can be found in Chapter 3.